18th International Conference on Structural Mechanics in Reactor Technology (SMiRT 18)
Beijing, China, August 7-12, 2005
SMiRT18-G11-1

MASTER CURVE ANALYSIS OF A GERMAN RPV STEEL CONSIDERING LOCAL CONSTRAINT

Dieter Siegele
Fraunhofer-Institute for Mechanics of Materials, Freiburg, Germany
Phone: +49761 5142-116, Fax: -401
E-mail: dieter.siegele@iwm.fraunhofer.de

Jörg Hohe
Fraunhofer-Institute for Mechanics of Materials, Freiburg, Germany
Phone: +49761 5142-116, Fax: -401
E-mail: joerg.hohe@iwm.fraunhofer.de

Valerie Friedmann
Fraunhofer-Institute for Mechanics of Materials, Freiburg, Germany
Phone: +49761 5142-116, Fax: -401
E-mail: valerie.friedmann@iwm.fraunhofer.de

ABSTRACT

The application of the master curve concept enables the testing of small specimens for the determination of a material fracture toughness curve to be used for the assessment of components. However, small specimens could have a larger plastic deformation preceding failure and therefore possibly different constraint situation than larger specimens or components. Within these investigations for a wide range of specimens with different constraint, the master curve reference temperature T_0 was determined and the correlation of the constraint on T_0 was quantified in terms of different two parameter concepts. In addition, fractografic and microstructural investigations as well as finite element analyses were performed to analyze the mechanisms and conditions of fracture initiation.

The investigations show a good agreement between the experimentally determined initiation sites and the location of maximum stresses. The different fracture mechanics specimen geometries investigated result in distinct differences in the reference temperature T_0 that correlate with the secondary fracture parameters T_{stress} or Q or h, respectively, at failure. Thus, the effect of the local constraint on the fracture toughness can be described by a shift of the reference temperature depending on the secondary fracture parameter. In addition the validity of ASME Code Cases N-629 and N-631 was proven.

Keywords: Master curve, constraint, fracture mechanism, fracture probability, stress analysis.

1. INTRODUCTION

The master curve concept developed by Wallin (1991) describes the probability of cleavage fracture of ferritic steels on the basis of the stress intensity factor K_J derived from the elastic-plastic J-integral. The failure probability is described by a three-parametric Weibull distribution in the form

$$P_f(K_J) = 1 - \exp\left(-\left(\frac{K_J - K_{\min}}{K_0 - K_{\min}}\right)^m\right) \tag{1.1}$$

where the materials parameter m and K_{min} are set to the constant values $m = 4$ and $K_{min} = 20$ MPam$^{1/2}$. The median fracture toughness K_{Jc}^{med} which corresponds to a fracture probability of 50% is determined according to the following equations with the reference temperature T_0 as material parameter:

$$K_{Jc}^{med} = K_{\min} + (K_0 - K_{\min})(\ln 2)^{1/4} \tag{1.2}$$

$$K_{Jc}^{med}(T) = (30 + 70\exp(0.019(T - T_0)/°C))MPam^{1/2} \tag{1.3}$$

Comparable to the ASME K_{IC}-curve the shape of the master curve is postulated to be the same for all ferritic steels. The advantage of the master curve is the direct determination of the reference temperature T_0 from fracture mechanics tests instead of the indirect estimation of RT_{NDT} from dynamic Charpy and Pellini tests as regulated in the ASME Code, Sec. XI (1995). Because of less stringent size requirements for the determination of valid K_{JC} values much smaller specimens can be used for the determination of the fracture toughness curve than for the ASME K_{IC}-curve that requires valid K_{IC}-test data according to ASTM E 399 (1989). K_{IC} is restricted to contained yielding, whereas for valid K_{JC}, more extended plasticity preceding cleavage is allowed. But due to comparable fracture mechanism, i.e. transgranular cleavage fracture, both quantities should be equivalent. For different data bases of RPV steels Siegele *et al.* (2005) showed that both K_{IC} and K_{JC} data result in the same master curve reference temperature T_0.

The probability of failure, i.e. the presence of a weak particle as triggering point for cleavage initiation depends on the material volume under high loading represented by the length of the crack front. According to the weakest link theory (see *e.g.* Beremin 1983, Mudry 1987), this behavior is considered in the master curve concept regulated in ASTM E 1921 (2003) by normalization of K_{JC} to a reference length of the crack front of 25 mm by the equation

$$K_{Jc}^{ref} = K_{\min} + (K_{Jc} - K_{\min})\left(\frac{b}{b_0}\right)^{1/4} \tag{1.4}$$

The adoption of the stress intensity factor *K* or the *J*-integral as a single fracture parameter is motivated by the fact that these parameters represent the first and dominant term of the expansion of the elastic crack tip field or the elastic plastic HRR field. Thus, they quantify the mechanical fields directly ahead of the crack front. On the other hand, it is experimentally observed that cleavage fracture originates not directly from the crack front but in the ligament in some distance ahead of the crack front. At this point, the higher order terms in the expansion of the mechanical fields might have a distinct effect on the stress state at the cleavage origin. The influence of these second order terms depend on the specimen and crack geometry as well as on the degree of plastic deformation. With increasing plastic deformation the constraint ahead of the crack front decreases with the consequence of an increase of fracture toughness (Siegele *et al.* 2002 and 2004, Hohe et al. 2005).

The most frequently used two parameter concept is the elastic *K*-T_{stress} concept (see *e.g.* Du and Hancock 1991), where the asymptotic crack tip stress field is given by

$$\sigma_{ij}(r,\varphi) = \frac{K}{\sqrt{2\pi}} r^{-\frac{1}{2}} f_{ij}(\varphi) + T_{stress}\, r^{0}\, g_{ij}(\varphi) \tag{1.5}$$

Here, the fracture toughness K together with the T_{stress} form the two parameter fracture toughness locus. Advantage of this concept compared to the corresponding one parameter concept in terms of K only is that the area of dominance for the asymptotic crack tip field is extended.

Whereas the K-T_{stress} concept uses a rigorous mathematical formulation, the J-Q concept (see *e.g.* O'Dowd 1995) simply employs the difference

$$Q = \frac{\sigma_{\varphi\varphi} - \sigma_{\varphi\varphi}^{ref}}{\sigma_0} \tag{1.6}$$

of the crack front stress field $\sigma_{\varphi\varphi}$ obtained in a finite element simulation and a reference stress field $\sigma_{\varphi\varphi}^{ref}$ normalized to the yield stress σ_0. Advantage of the J-Q concept is that it can address both, the in-plane constraint due to a cleavage origin at a finite distance ahead of the crack tip as well as the effect of constrained transverse deformation along the crack front.

In an extensive research program (see Hohe *et al.* 2005), the applicability of the master curve concept is investigated for a German RPV steel under consideration of the influence of local constraint on fracture toughness. The tests are simulated with the aid of finite elements in order to quantify the local conditions for cleavage crack initiation and the influence factors such as volume of high stressed material and local constraint. The effect of different stress states in the vicinity of the crack front for the different specimen types was quantified in terms of the different two parameter concepts, especially the K-T_{stress} and J-Q approaches.

In addition, fractografic and microstructural investigations are performed to analyze the mechanisms of fracture initiation and extension.

2. MATERIAL AND METHODS

The material investigated is a German 22 NiMoCr 37 (A 508 Class 2) rector pressure vessel steel. The fracture toughness of the material is determined using a variety of fracture mechanics specimens including Charpy sized SE(B)10x10 specimens with three different crack depths ($a/w \approx 0.51$, $a/w \approx 0.18$ and $a/w \approx 0.13$), C(T) specimens with different sizes (C(T)25 and C(T)50, both with $a/w \approx 0.51$) as well as center cracked CC(T)100 specimens with $2a/w \approx 0.51$. All specimens are tested displacement controlled under quasi static loading. The test temperatures are varied between T = -120°C and T = 0°C. The fracture toughness is determined according to ASTM Standard E 1921-03 (2003). For the shallow cracked SE(B)10x10 specimens, the plastic correction factor in the approximate formulae given in ASTM E1921 is adjusted such that the obtained approximation for the average J-integral matches with the value obtained from a finite element analysis of the test (see Section 3) using its definition as a path independent integral around the crack front. The fracture toughness for the CC(T) specimens is obtained in a similar manner. All toughness results are normalized to a crack front length of B = 25 mm as required in ASTM E 1921 (2003).

After testing, the fracture surfaces were investigated and the locations of the fracture initiation sites were determined using a scanning electron microscope. With the aid of finite elements analyses the stress fields ahead of the crack tip were analyzed with respect to the conditions for cleavage initiation under consideration of the local constraint situation.

3. FRACTURE TOUGHNESS RESULTS

The experimental results are presented in Fig 1. The master curve reference temperature evaluated from the standard deeply notched specimens with high constraint as required in ASTM E1921 is determined to be T_0 = -65.4°C. It is observed that most of the experimental results are enveloped by the 5% and 95% fractiles of the master curve. But besides two data points below the 5% curve a significant amount of data points are above the 95% fractile. Especially, fracture toughness values K_{Jc} obtained from the CC(T)100 specimens tested at T = -90°C as well as the fracture toughness values obtained from the shallow crack SE(B)10x10 specimens with $a/w \approx 0.13$ exceed the prediction of a failure probability of P_f = 95% as predicted by the master curve concept.

The separate evaluation of CC(T)100 and shallow crack SE(B) specimens is illustrated in Fig. 2. The reference temperature T_0 determined from the CC(T) specimens is found to be -105.3°C which is about 40°C lower than the average value of all deeply cracked specimens. For the SE(B)10x10 specimens with a/w=0.13, T_0 is determined to be -92.7°C which is a shift of about 27°C to lower temperatures. The correlation between T_0 and the level of constraint characterized by several constraint parameters is discussed in chapter 5.

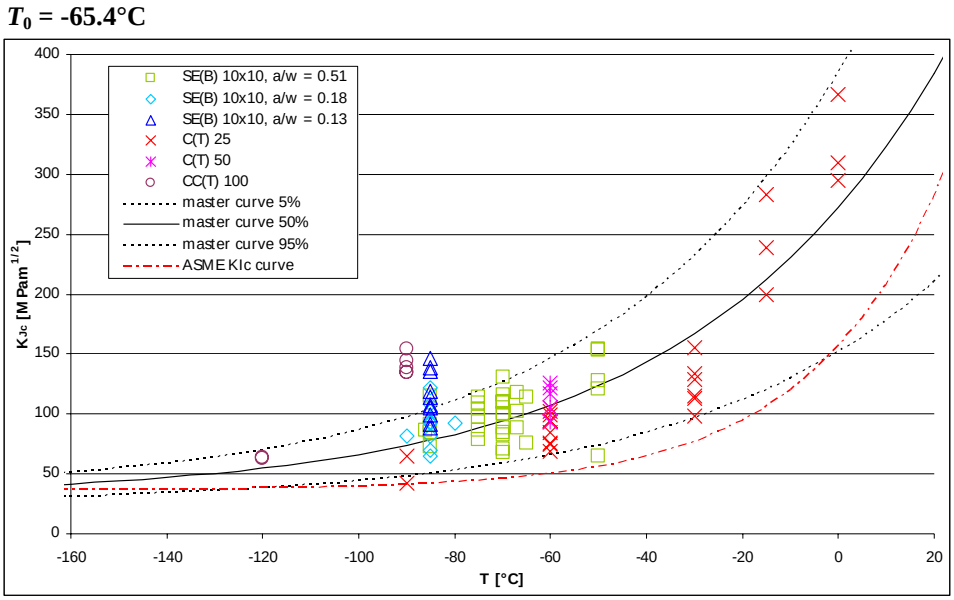

Fig. 1. Fracture toughness results with the master curve determined from the deeply notched specimens (T0= -65°C) as well as the ASME KIC curve adjusted to RTTo=T0+19.4°C

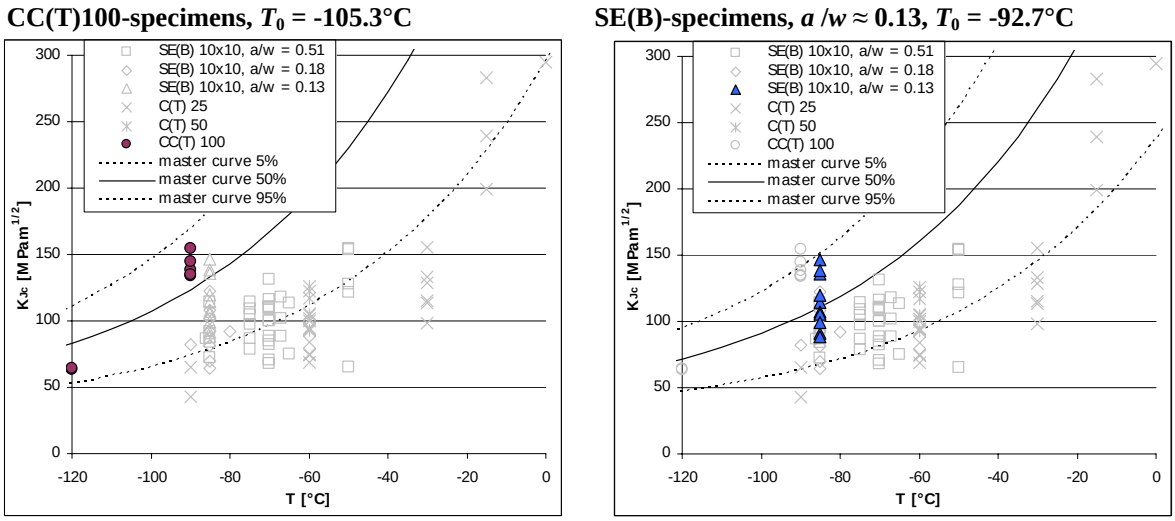

Fig. 2. Master curve analysis from the CC(T)100- and the shallow cracked SE(B)-specimens

The ASME Code Cases N-629 and N-631 (1999) allow the use of fracture toughness data to establish a fracture-toughness-based reference temperature RT_{To} as an alternative and functional equivalent to the reference temperature RT_{NDT} to adjust the ASME K_{IC}-lower bound curve on the temperature axis. RT_{To} is based on the master curve reference temperature T_0 and adjusted to the 5% master curve with the intersection point at K_{JC} of

150 MPam$^{1/2}$ according to $RT_{To} = T_0 + 19.4°C$. This adjusted K_{IC}-curve is also plotted in Fig. 1. It is shown that all fracture toughness data are enveloped by the ASME K_{IC}-curve adjusted to RT_{To}. This result is in accordance with Server and Rosinski (1998) and Keim *et al.* (2005).

As often discussed in literature [see *e.g.* Joyce 2000, Wallin *et al.* 2001] and introduced in the newest version of ASTM E 1921-03, bending specimens could result in lower T_0 values than C(T)-specimens. The separate evaluation of T_0 from SE(B)10x10 and C(T)25 specimen results is plotted in Fig. 3. As expected, T_0 determined from SE(B) specimens is some 10°C lower compared to T_0 from C(T) specimens. This is in accordance with ASTM E 1921 in which a margin between 10°C and 15°C was proposed.

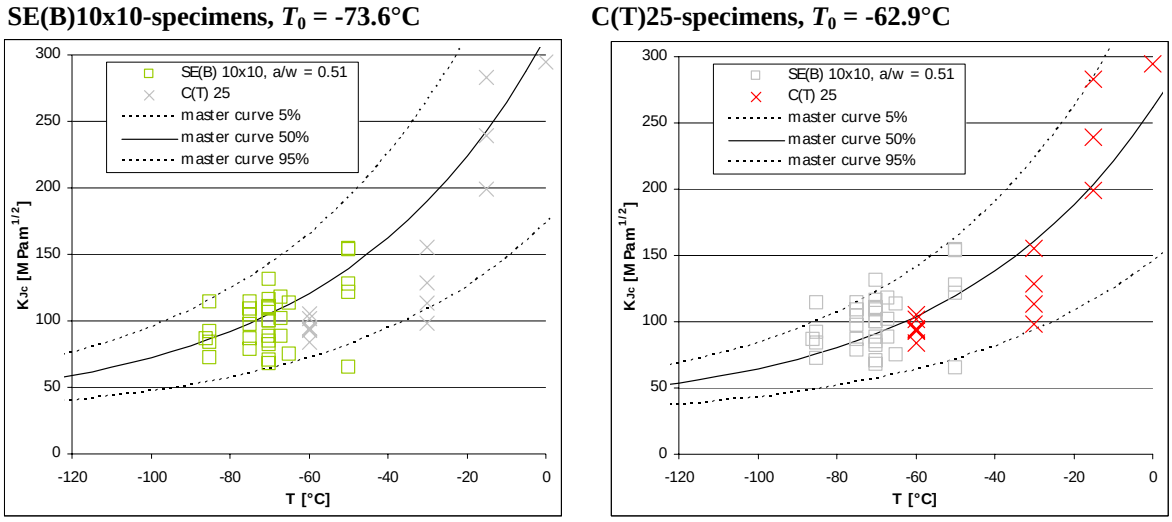

Fig. 3. Master curve analysis from the SE(B)10x10- and the C(T)25-specimens

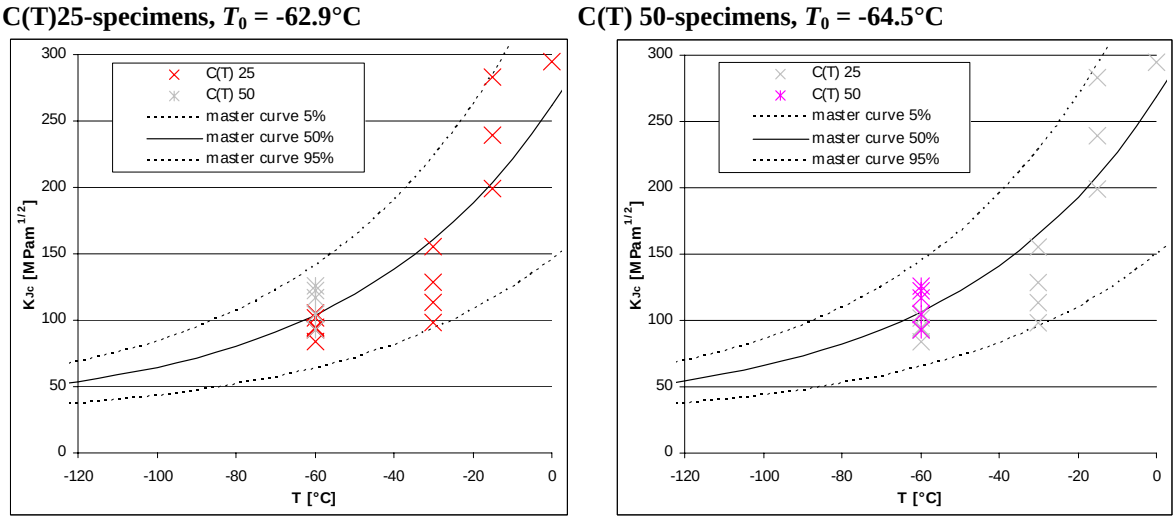

Fig. 4. Master curve analysis from the C(T)25- and the C(T)50-specimens

Fig. 4 shows the comparison of T_0 evaluations from C(T)25 and C(T)50 specimens. Although only 5 C(T)50 specimens have been tested (one less than required in ASTM E 1921) the results are very close which is a further confirmation of the validity of the size correction of K_{JC} based on the assumption of the weakest link model.

4. INVESTIGATION ON FRACTURE MECHANISMS

The master curve concept allows the testing of small specimens that could have a considerable amount of plastic deformation and some ductile crack extension (5% of the ligament) preceding final cleavage fracture. For the transferability of the fracture toughness curve determined from small specimens to components the fracture mechanisms for the specimens have to be comparable independent of specimen geometry. With the aid of investigations of fracture surfaces using scanning electron microscope as well as by interrupted tests the development and the mechanisms of fracture for different specimens have been analyzed.

As an example, Fig. 5 shows the fracture surfaces of a C(T)50 compared to a SE(B)10x10 specimen. It is clearly visible that for both specimens the fracture mechanism at initiation site is the same, namely pure transgranular cleavage although the C(T)50 specimen failed in the linear elastic regime at a valid K_{IC} value whereas the failure of the SE(B) specimen is described by K_{JC}. Both specimens failed at a comparable K-value of about 100 MPam$^{1/2}$ at nearly the same test temperatures (C(T)50: -60°C, SE(B)10x10: -67°C).

C(T)50-specimen, T= -60°C, K_{IC}=102 MPam$^{1/2}$ **SE(B)10x10-specimen, T= -67°C, K_{JC}=106 MPam$^{1/2}$**

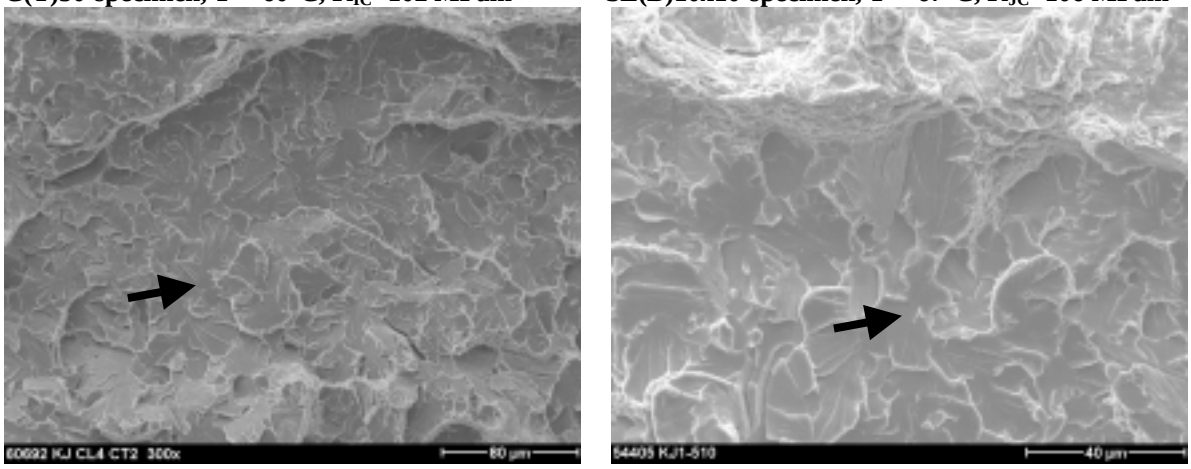

Fig. 5. Fracture surfaces of a C(T)50-specimen failed at K_{IC}=102 MPam$^{1/2}$ and a SE(B)-specimen failed at K_{JC}=106 MPam$^{1/2}$, initiation sites marked by arrows.

In the brittle/ductile transition range, brittle failure occurs after plastic deformation of the crack tip (blunting) which can be accompanied with increasing load by some local ductile damage and crack extension. In order to investigate the different stages of damage during loading, interrupted tests on SE(B)10x10 specimens were performed at a test temperature of -50°C where the specimens were loaded up to different load levels without failing. After unloading, the specimens were cut along the centerline perpendicular to the crack plane and were prepared for visualization of the crack tip opening and the evolution of damage (void nucleation and growth, coalescence of voids).

Fig. 6 shows the cuts of two specimens loaded up to a K-value of 135 and 170 MPam$^{1/2}$, respectively. At the lower load level, the blunting of the crack tip and some first small voids ahead of the crack tip are visible. For the specimen interrupted at the higher load, larger ductile voids and some first coalescence of voids resulting in local crack extension of some micrometer can be observed. From observation of the whole fracture surface it can be noted, that even at the highest load level the ductile crack extension is very little and not homogeneous along the crack front but occurs only locally.

On the other hand, the fracture toughness results of the SE(B)10x10-specimens tested at -50°C show a large scatter of K_{JC} ranging from 77 to 190 MPam$^{1/2}$. Due to limitation of the specimen size according to ASTM E 1921, K_{JC} has to be censored to a value of about 135 MPam$^{1/2}$. Therefore, the small local ductile crack extension only occurs in specimens with censored fracture toughness results.

SE(B)10x10-specimen, T= -50°C, K_J=135 MPam$^{1/2}$ **SE(B)10x10-specimen, T= -50°C, K_J=170 MPam$^{1/2}$**

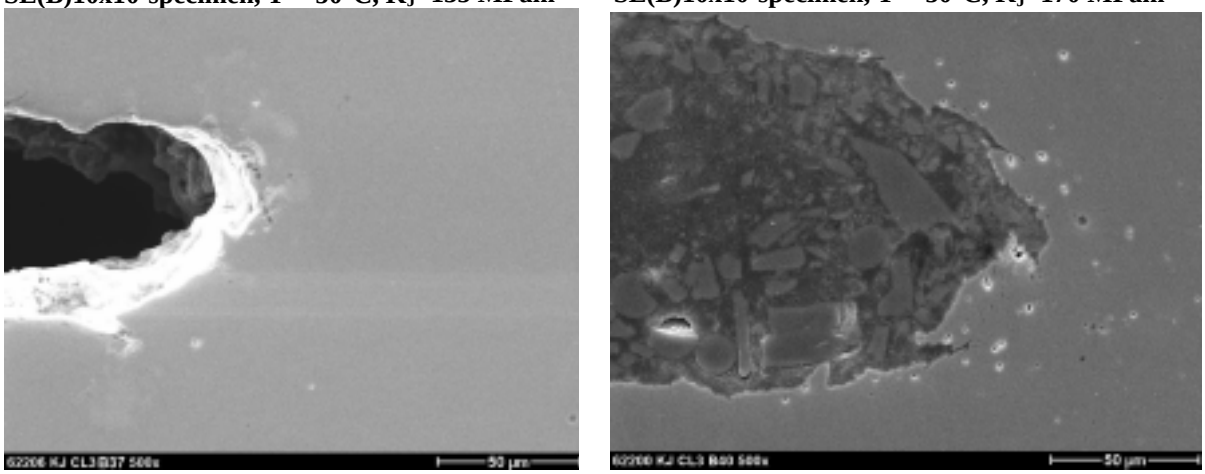

Fig. 6. Evolution of crack tip blunting and damage (void nucleation, growth and coalescence) evaluated on SE (B) 10x10-specimens interrupted at different load levels

C(T)25-specimen, T= -15°C, K_{JC}=283 MPam$^{1/2}$

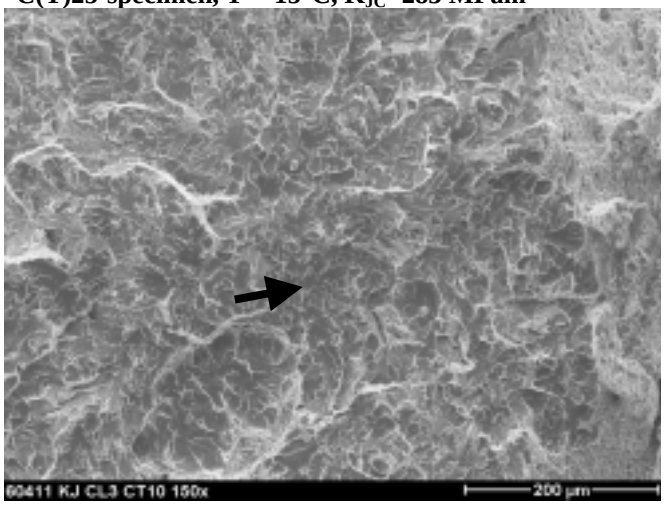

Fig. 7. Fracture surface of a C(T)25-specimen failed at K_{JC}=283 MPam$^{1/2}$, initiation site marked by arrow.

For C(T) specimens however, fracture toughness tests at higher temperature up to higher loads were performed. Fig. 7 shows the fracture surface of a C(T)25 specimen tested at -15°C which failed at a K_{JC} value of 280 MPam$^{1/2}$ with prior ductile crack extension of about 0.3 mm. The fracture mechanism is also transgranular cleavage initiated at a distance of about 0.26 mm from the ductile crack front.

From the microstructural investigations it can be concluded that all specimens which failed by brittle fracture show the same fracture mechanism at initiation site being transgranular cleavage independent of ductile deformation or crack extension. Homogeneous ductile crack extension along the crack front occurs only in specimens tested at K_{JC} values above 200 MPam$^{1/2}$. Such loads was only applied on C(T) specimens at test temperatures above -15°C. However, these test temperatures are about 50°C above T_0 or higher and the test results have not to be considered in the T_0 estimation.

5. ANALYSIS OF LOCAL STRESS FIELDS

In order to analyze the effect of the local mechanical fields on the triggering of cleavage fracture for the different types of specimens, elastic plastic finite element analyses of all fracture mechanics tests were performed, using detailed three-dimensional models with an extremely high mesh resolution in the vicinity of the crack front.

The most important field quantity is the maximum principal stress ahead of the crack front which is assumed to be responsible for the initiation of micro defects nucleated during the plastic deformation of this region. In Fig. 8, the distribution of the maximum principal stress is presented for a typical deep cracked SE(B)10x10 specimen (Fig. 8a) and a typical C(T)25 specimen (Fig. 8b) tested at a similar temperature. In order to enable a more distinct understanding of the stress situation, the "true" Cauchy stress related to the actual configuration is considered. Five different load levels are considered, where the maximum load level corresponds to the failure load of the respective specimen. The cleavage origins obtained from the fractographic analyses are marked as dashed lines.

At all load levels, the maximum principal stress increases from the crack front towards a maximum value in a short distance ahead of the crack front. Further away, the maximum principal stress decreases monotonically. In both cases, cleavage fracture originates from a point in the vicinity of the maximum of the stress distribution. For both specimens considered in Fig. 8, as well as for all other specimens investigated, at the cleavage origin similar levels of the maximum principal stress are obtained being about 1800 MPa for this material. Thus, the maximum principal stress forms a suitable local criterion for the initiation of cleavage fracture. On the other hand, it is obvious that the maximum principal stress reaches the corresponding critical value already in an early stage of the loading history at a spatial position close to the crack front. Although a local fracture criterion based on the maximum principal stress would be satisfied in those cases, no cleavage fracture is initiated at these sites for low load levels. This effect might be explained by the fact that cleavage fracture always originates from weak zones in the vicinity of particles and inclusions in the material. Thus, a necessary local criterion for cleavage fracture requires both, a reasonable high local stress as well as the presence of a weak point at the same location. Since the particles and inclusions are distributed randomly through the material, the probability of cleavage initiation increases, if the area where high local stress levels are reached increases as it does with increasing external load (see Fig. 8).

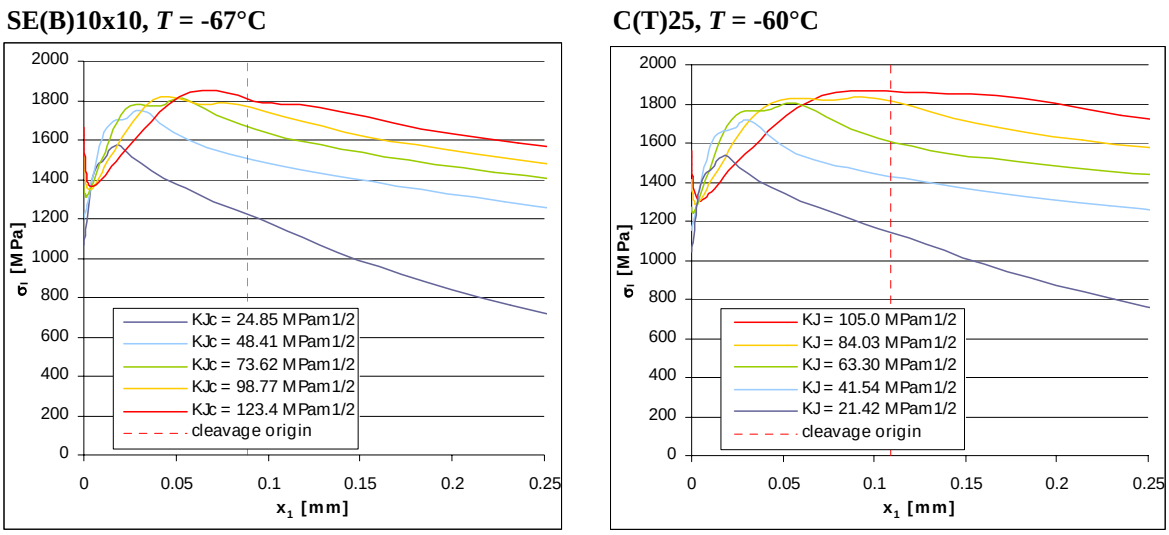

Fig. 8. Distribution of maximum principal stress within the ligament

Another important field quantity governing the initiation of cleavage fracture is the local stress triaxiality (constraint). At low constraint, freshly nucleated micro defects are likely to blunt and thus to become undercritical whereas large stress triaxialities might result in a more critical situation without blunting of the micro defects. The distribution of the local stress triaxiality coefficient $h = \sigma_{kk}/(3\sigma_e)$ is presented in Fig. 9, considering the same specimens and load levels as in Fig. 8. It is observed that, similar as in the distributions of the maximum principal stress, the stress triaxiality reaches its maximum in the vicinity of the cleavage origin. The numerical value of the

maximum remains constant through a long part of the loading history, however, the location of the maximum is shifted from the crack front into the ligament if the external load is increased. Comparing the maximum values of the triaxiality coefficient for both specimen geometries, it is observed that somewhat larger values are attained for the C(T) specimens. Thus, the triaxiality coefficient *h* might serve as a parameter to characterize the crack front constraint situation of different specimen geometries.

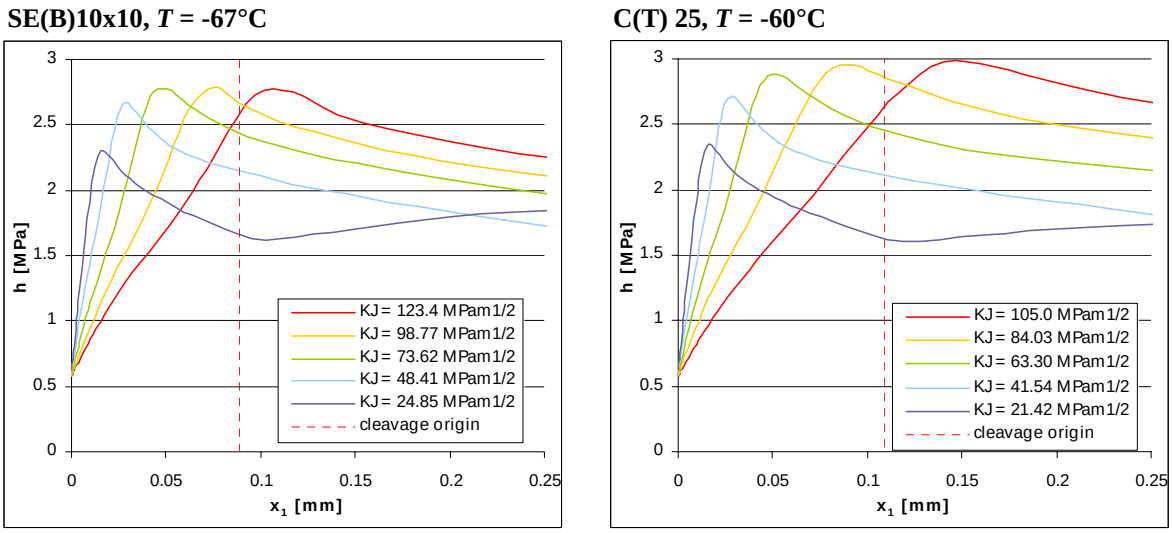

Fig. 9. Distribution of stress triaxiality coefficient within the ligament

6. ASSESSMENT OF CONSTRAINT

In order to investigate the effect of the crack front constraint in more detail, the secondary fracture parameters for two different two parameter concepts are determined for all specimens tested. In this context, the K-T_{stress} and the J-Q approaches are employed. Furthermore, the loss of thickness constraint for thin specimens at higher load levels is addressed.

In these analyses, the elastic T_{stress} is determined from the numerical results of an elastic finite element analysis using the interaction integral implemented in the finite element code ABAQUS (2004). The Q parameter is determined as the difference between the circumferential stresses obtained in the elastic plastic finite element analysis of the respective fracture mechanics experiment and the circumferential stress for a reference crack tip field. The reference stress field is a plane strain field for the problem of a semi infinite crack in an infinite medium with the same material properties as for the material used in the experiments. The reference stress field is determined numerically in a boundary layer analysis under prescribed displacements according to the J-integral obtained in the corresponding fracture experiment. The stresses are evaluated in the centre of the ligament at a distance of $r = 2J/\sigma_0$ from the crack front.

In Fig. 10, the results for the secondary fracture parameters at failure of all specimens tested are presented, concerning both, the T_{stress} normalized by the temperature dependent yield stress σ_0 and the Q parameter. For the different specimen geometries different levels of the secondary fracture parameters T_{stress}/σ_0 and Q are obtained which are unique for the respective specimen geometry irrespectively of the test temperature. An exception are the two CC(T)100 specimens tested at T = -120°C which failed at an extremely low external load level.

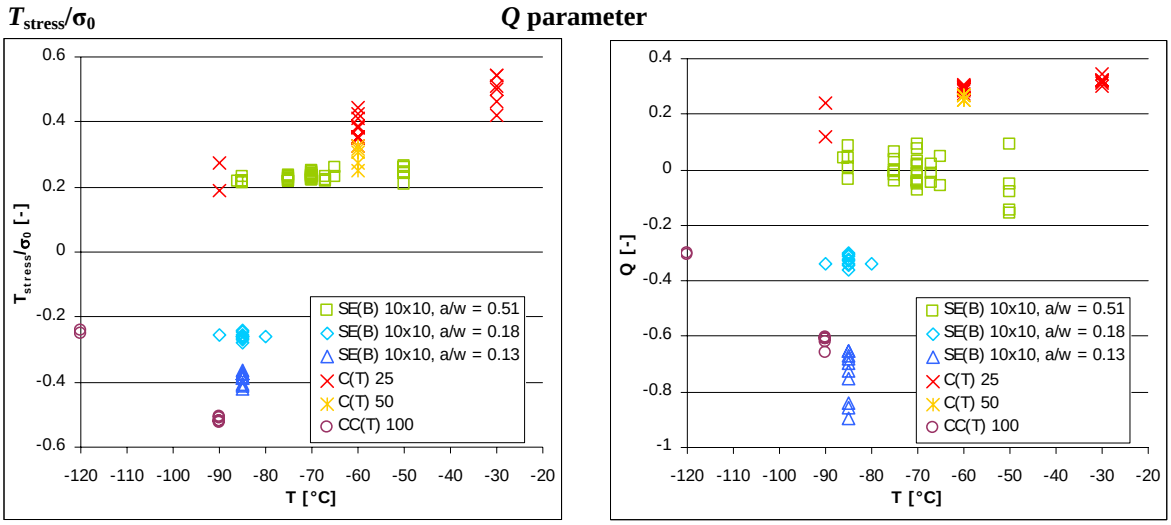

Fig. 10. Secondary fracture parameters for all specimens

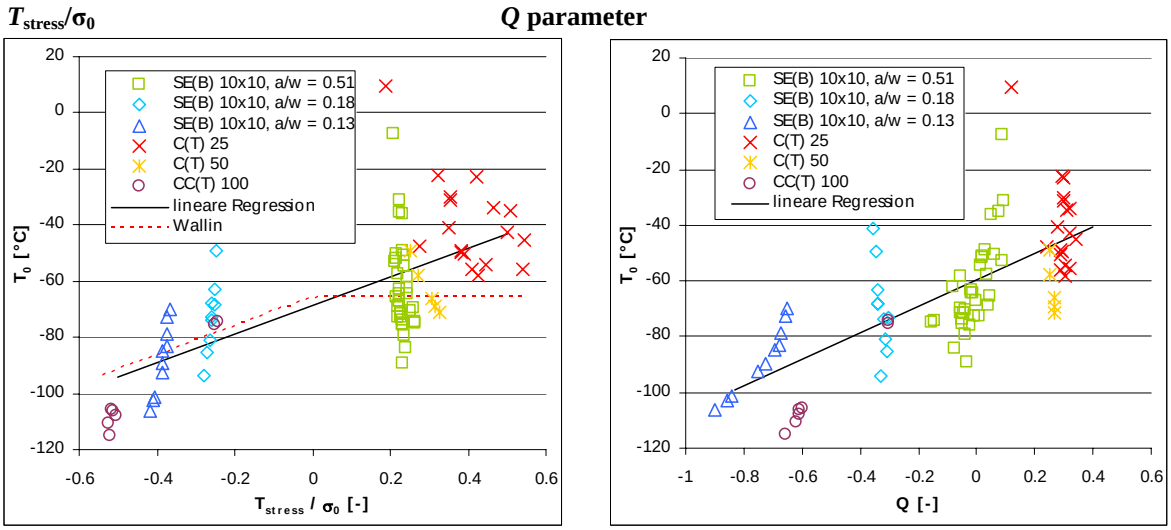

Fig. 11. Effect of the secondary fracture parameters on the master curve reference temperature

The effect of the secondary fracture parameters on the master curve reference temperature T_0 is investigated in Fig. 11. In order to be able to assess the scatter of the results in both, the fracture toughness as well as the secondary fracture parameters, an individual reference temperature has been determined for all tests performed. It is observed that the scatter in the secondary fracture parameter is in general less than the scatter in the fracture toughness or the master curve reference temperature respectively. For both two parameter concepts considered, the effect on the reference temperature T_0 can be approximated by a linear function as it has been suggested earlier by Wallin (2001). His proposal for a constraint correction of the reference temperature according to

$$T_0 = T_0^{ref} + \frac{T}{10}\frac{°C}{MPa} \quad , \qquad T \le 0 \tag{6.1}$$

is found in a good agreement with the present experimental data. Thus, the effect of the local crack front constraint on the fracture toughness can be described by a shift of the reference temperature depending on the secondary fracture parameter.

The linearly constraint dependent shift of the master curve reference temperature T_0 is in general a convenient and easy to use possibility for inclusion of the constraint effect into the master curve concept. On the other hand, this procedure results in the definition of a material parameter (T_0), which depends on the local loading situation (in terms of the respective secondary fracture parameter) which is not only unsatisfactory from the theoretical point of view but also causes problems in the determination of T_0 from mixed data sets. An alternative could be to perform the shift not in terms of the reference temperature T_0 but in the test or service temperature T defining a constraint neutral reference temperature, similar to the thickness correction of the fracture toughness. Both approaches are identical since the master curve depends on $T - T_0$. Nevertheless, in this case the assessment of transient service conditions would be difficult since the constraint situation might vary due to plastic deformation during the loading process. A possibility to avoid the problems with both approaches for a constraint correction consists in the definition of a constraint correction to the fracture toughness by relating all stress intensity factors to a reference case similar to the thickness correction to a reference thickness of 25 mm.

Since the master curve is defined by an exponential function, a shift of its graph with respect to its argument coincides with a scaling of the graph. Thus, a scaling of the fracture probability according to

$$K_{Jc}(T,Y) = \left(20 + \left(10 + 70e^{0.019\left(T - T_0 + c\left(Y^{ref} - Y\right)\right)} \right) \left(-\frac{\ln(1-P_f)}{\ln 2} \right)^{1/4} \right) MPam^{1/2} \tag{6.2}$$

coincides with a linearly constraint dependent temperature shift. In this equation, the symbol Y denotes the respective secondary fracture parameter whereas c is the slope of the linear temperature correction. For the present experimental data base, the correction parameters are listed in Table 1. Similar to the thickness correction, the case of the C(T)25 specimen is chosen as the reference case.

Table 1. Parameters for the constraint correction

Y	c	Y^{ref}
T_{stress}	0.093°C/MPa	195.5 MPa
T_{stress}/σ_0	50.74°C	0.403
Q	48.45°C	0.290

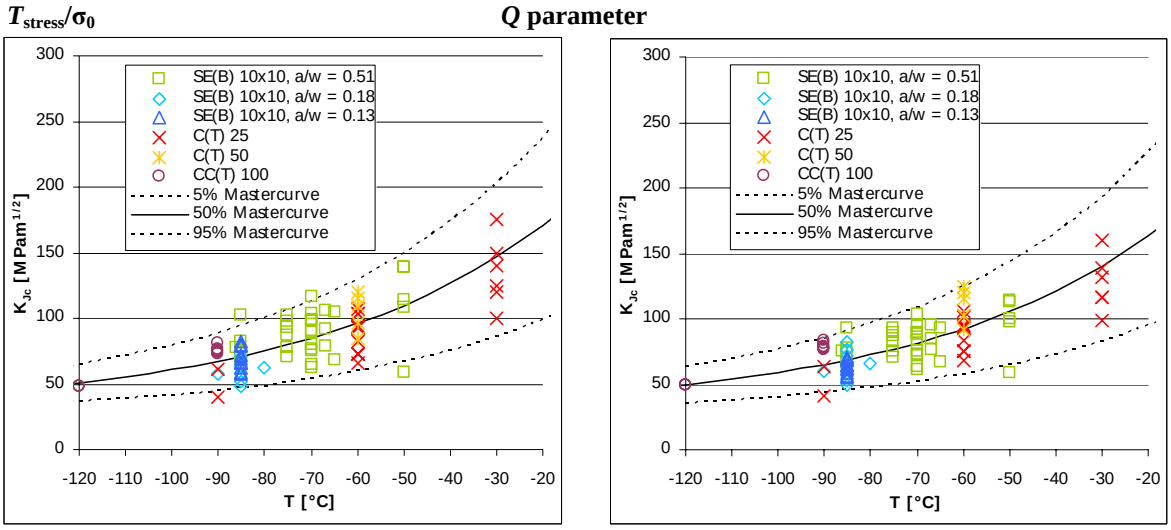

Fig. 12. Constraint correction by a constraint dependent scaling of the fracture toughness

In Fig. 12, the constraint correction defined above is applied to the present experimental data base using both the K-T_{stress} and the Q concept. It is observed that in both cases, most of the data points are enveloped by the 5%- and 95% fractiles of the master curve concept with constraint neutral reference temperatures of T_0^{cn} = -56.9°C and T_0^{cn} = -53.9°C, respectively. In this context, it should be noticed that the constraint neutral master curve reference temperature T_0^{cn} is related to the reference case of the C(T)25 specimens and not comparable to the reference temperature T_0 of the original concept.

For the K-T_{stress}-concept, 6% of the data are below or beyond the 5%- and the 95%-fractile, whereas 4.8% of the data are not within this area in case of the J-Q-concept. Thus, less than 10% of the data is found outside the envelope. Therefore, the proposed constraint correction of the stress intensity factures provides a suitable method to obtain transferable fracture parameters.

7. CONCLUSIONS

Within the framework of a German reactor safety research programme the applicability of the master curve concept was investigated for a German RPV steel under consideration of the influence of local constraint on fracture toughness. The investigations cover a wide range of tests on C(T), SE(B) and CC(T) specimens with different overall sizes and crack depths. The tests were evaluated according to the master curve concept to determine the reference temperature T_0 according to ASTM E 1921-03. In addition, fractografic and microstructural investigations were performed to analyze the mechanisms of fracture initiation and extension.

The tests were simulated with the aid of finite elements in order to quantify the conditions for cleavage crack initiation and the influence factors such as magnitude of highly stressed material volume and local constraint. The effect of different stress states in the vicinity of the crack front for the different specimen types was quantified in terms of different two parameter concepts.

The comparison of experimentally determined initiation sites and the calculated local stress fields show a good correlation between the crack initiation site and the location of the maximum principal stresses. The different fracture mechanics specimen geometries result in distinct differences in the fracture toughness that correlate with the secondary fracture parameters T_{stress} or Q, respectively, at failure. A determination of an individual master curve reference temperature for all single experiments shows an approximately linear relationship between the reference temperature and the corresponding constraint parameter. Thus, the effect of the local constraint on the fracture toughness can be described by a shift of the reference temperature depending on the secondary fracture parameter. The microstructural investigations reveal that all specimens show the same fracture mechanism at initiation site namely transgranular cleavage independent of ductile deformation or crack extension. Ductile crack extension

along the whole crack front is only observed for specimens tested at K_{JC} values above 200 MPam$^{1/2}$. Only 2% of the specimens tested result in fracture toughness K_{JC} below the 5% master curve. All test results are enveloped by the ASME K_{IC} curve according to ASME Code Cases N-629 and N-631.

ACKNOWLEDGEMENT

The investigations have been performed within the framework of the reactor safety research project no. 150 1239 supported by the German Ministry of Economics and Labour (BMWA).

REFERENCES

ABAQUS/Standard, "User's Manual, Version 6.5", ABAQUS, Inc., Providence, R.I, 2004

ASME Boiler and Pressure Vessel Code Sec XI, American Society of Mechanical Engineers, New York, 1995

ASME Code Case N-629, Use of Fracture Toughness Test Data to Establish Reference Temperature for Pressure Retaining Materials, Sec. XI, Division 1, 1999

ASME Code Case N-631, Use of Fracture Toughness Test Data to Establish Reference Temperature for Pressure Retaining Materials Other than Bolting for Class 1 Vessels, Sec. III, Division 1, 1999

ASTM Standard E 399-83: Standard Test Method for Plane Strain Fracture Toughness of Metallic Materials, Annual Book of ASTM Standards, American Society for Testing and Materials, Philadelphia, PA, 1989

ASTM Standard E 1921-03: Standard Test Method for Determination of Reference Temperature T_0 for Ferritic Steels in the Transition Range. ASTM International, West Conshohocken, PA, 2002

Beremin, F.M.: A Local Criterion for Cleavage Fracture of a Nuclear Pressure Vessel Steel, Metall. Trans. 14A, 2277-2287, 1983

Du, Z.Z. and Hancock, J.W.: The Effect of Non-Singular Stresses on Crack-Tip Constraint, J. Mech. Phys. Solids 39, 555-567, 1991

Hohe, J., Hebel, J. and Siegele, D., Two Parameter Approaches in the Probabilistic Failure Assessment of Ferritic Steels, ICF XI, 11th International Conference on Fracture, Turin March 20-25, 2005

Hohe, J. et al., Kritische Überprüfung des Mastercurve-Ansatzes im Hinblick auf die Anwendung bei deutschen Kernkraftwerken, Fraunhofer IWM, Report S8/2004, 2005.

Joyce, J. and Tregonning, R., Quantification of Specimen Geometry Effect on the Master Curve and T0 Reference Temperature, ECF 13, Fracture Mechanics: Applications and Challenges, Elsevier Science, 2000

Keim, E., Siegele, D. and Nagel, G., Validation of RT_{To} for German Reactor Pressure Vessel Steels, PVP2005-71197, ASME Pressure Vessels and Piping Division Conference, Denver, Colorado, USA, July 17-21, 2005

Mudry, F., A Local Approach to Cleavage Fracture, Nucl. Eng. Des. 105, 65-76, 1987

O'Dowd, N.P.: Applications of Two-Parameter Approaches in Elastic-Plastic Fracture Mechanics, Eng. Frac. Mech. 52, 445-465, 1995

Server, W.L. and Rosinski, S.T., Technical Basis for Application of the Master Curve Approach to Reactor Pressure Vessel Integrity Assessment, Effects of Radiation on Materials, 19th International Symposium, ASTM STP 1366, Seattle, 1998

Siegele, D., Varfolomeyev, I. and Nagel, G.: Constraint based Assessment of postulated nozzle corner cracks, 2002 ASME Pressure Vessels and Piping Conference, Vancouver, BC, August 04-08, 2002

Siegele, D., Varfolomeyev, I., Wallin, K. and Nagel, G.: Investigation of Constraint Effects on Fracture Toughness for CC(T) Specimens, 2004 ASME Pressure Vessels and Piping Conference, San Diego, CA, July 25-29, 2004

Siegele, D., Keim, E. and Nagel, G., Comparison of Reference Temperature T_0 from Instability K_{Jc} and K_{Ic} Fracture Toughness, PVP2005-71346, ASME Pressure Vessels and Piping Division Conference, Denver, Colorado, USA, July 17-21, 2005

Wallin, K.: Statistical Modelling of Fracture in the Ductile-to-Brittle Transition Range, Defect Assessment in Components, Fundamentals and Applications (Blauel, J.G. and Schwalbe, K.H., eds.), Mechanical Engineering Publications, 415-445, London 1991

Wallin, K., Planman, T., Valo, M. and Rintamaa, R., Applicability of Miniature Size Bend Specimens to Determine the Master Curve Reference Temperature T_0, Engng. Frac. Mech. 68, 1265-1296, 2001

Wallin, K.: Quantifying T-Stress Controlled Constraint by the Master Curve Transition Temperature T_0, Eng. Frac. Mech. 68, 303-328, 2001

